DOI 10.1007/s10891-019-02028-z

Journal of Engineering Physics and Thermophysics, Vol. 92, No. 5, September, 2019

MODELING THE INDUCTION HEATING OF PRESS EQUIPMENT IN AN AUTOMATIC-TEMPERATURE-CONTROL MODE

A. O. Glebov, S. V. Karpov, S. V. Karpushkin, and E. N. Malygin

UDC 62-932.4

Consideration has been given to the most widespread three-dimensional formulations of a mathematical model of the process of inducing eddy currents in ferromagnetic materials. Two procedures have been proposed to calculate temperature fields of induction heating devices in a mode of automatic proportional-integral-differential temperature control, which makes it possible to considerably reduce the consumption of computer time with ensuring acceptable accuracy. The first procedure provides for a successive conduct of electromagnetic and thermal analyses with the "scaling" of heat releases from the eddy currents at the stage of control. In the case of shortage computational resources it is possible to use the second procedure which involves a thermal model under the assumption of a uniform release of heat in the region of inductors and is only applicable for the inductors placed inside heated bodies. Using the calculation of temperature fields in press plates, molds, and vulcanized products as an example, the authors have shown the necessity of taking account of the period of stabilization of a temperature field in developing and operating heating plates.

Keywords: *induction heating, press equipment, eddy currents, PID controller, temperature field, finite-element analysis.*

Introduction. In the segment of press equipment intended for fabricating rubber technical goods (RTGs), the induction technique of heating of plates is preferred because of the durability of heating elements, i.e., inductors. The high indices of specific power make it possible to decrease the total length of grooves for placing them, to improve the manufacturability of a plate′s structure, and to provide a greater scope for optimizing the temperature field.

In the operating cycle of heating plates, we can single out two stages: 1) heating from the initial temperature to an assigned one and 2) automatic temperature control using a positioning controller or a proportional-integral-differential (PID) controller. At the second stage, the temperature field of a plate undergoes substantial changes produced by the reduction in the power consumption. In this connection, solution of problems of searching for optimum modes of implementation of the vulcanization process (assigned value of the temperature of a checking thermocouple, the vulcanization time, and also the duration of stabilization of the temperature field, i.e., reaching a nearly stationary temperature mode) assumes the conduct of thermal analysis at the stage of automatic control.

The difficulty with controlling the process of induction heating is due to the nonlinearity and nonstationarity of the electromagnetic processes underlying them (because of the presence of hysteresis). Furthermore, attaining assigned parameters of the temperature field of the working surface of a plate is made difficult by the intricate configuration of the temperature distribution in its volume, and also by perturbations of electromagnetic and thermal nature.

Scientific publications on the subject of control of the process of induction heating are mainly devoted to the development of methods and algorithms to synthesize the control of the existing technological objects. Here, these problems are solved without mathematical modeling of the temperature fields of objects based on consideration of integral indices, i.e., temperatures at one or several points, and investigation reliability is confirmed by the results of laboratory and simulation investigations.

The procedure of calculation of temperature fields of induction heating devices with positioning control was considered in [1]. An analysis of the results presented in this publication and others has shown that positioning control often fails to meet requirements imposed on the quality of control. For example, in controlling the induction heating of a system of molds for pressure molding of plastic, it is expedient to use only PID control [2].

Tambov State Technical University, 106 Sovetskaya Str., Tambov, 392000, Russia; email: karp@mail.gaps.tstu.ru.
Translated from Inzhenerno-Fizicheskii Zhurnal, Vol. 92, No. 5, pp. 2168–2179, September–October, 2019. Original article submitted February 6, 2018.

In automatic PID control, it is necessary to recalculate the values of heat releases from eddy currents for each instant of time, which strongly increases the amount of computations. In [3], it has been shown that the use of a regular PID controller is unacceptable in some cases and has been proposed that a controller based on fuzzy logic be used.

Mathematical Model of Induction Heating of Ferromagnetic Materials. The process of propagation of eddy currents in ferromagnetic materials is modeled by Maxwell′s fundamental equations whose direct solution in a three-dimensional formulation seems impossible. The development of mathematical models of propagation of eddy currents in three-dimensional bodies that are suitable for practical use began in the 1970s [4] and has not lost its relevance to date [5]. Over this period, a few mathematical models have been proposed whose solution with the finite-element method satisfies Maxwell′s initial differential equations. The models most widespread in calculation practice are as follows:

1) based on the vector magnetic potential **A** (Wb/m) and the scalar electric potential V (V) in a classical nodal formulation of the finite-element method [6];
2) based on the edge vector magnetic potential **A** and the nodal scalar electric potential V [7];
3) based on the edge vector current potential **T** (A/m) and the scalar nodal electric potential φ (A) [4, 7].

In [7, 8], it has been shown that approximation of the vector magnetic potential **A** by nodal basis functions at substantial values of the normal component of **A** at the boundaries of abrupt change in the magnetic permeability may lead to great errors in calculating eddy currents. Physically, the normal component of the vector magnetic potential at these boundaries undergoes a discontinuity which cannot be modeled using nodal finite elements. At present, the model based on the nodal vector magnetic potential loses its relevance for three-dimensional problems. Therefore, the support of finite elements SOLID97 of the ANSYS finite-element-analysis system, which implement this model, was stopped in 2016.

The use of edge basis functions makes it possible to ensure the discontinuity of the normal component of the vector magnetic potential. In this approximation, variables (degrees of freedom) are assigned by the edges of finite elements, not by their nodes. Let us consider this model in greater detail. In the space where an electromagnetic field is modeled, we can single out three domains: the existence domain of eddy currents Ω_1, the domain with zero electrical conductivity Ω_2 (air space or electrical insulation), and the domain with an external current Ω_3 (coil connected to a current or voltage source) (Fig. 1).

For the domain Ω_1, the mathematical model based on the edge vector magnetic potential and on the scalar electric potential is of the form

$$\text{rot}\ (\mu^{-1}\ \text{rot}\ \mathbf{A}) + \gamma\ \frac{\partial \mathbf{A}}{\partial t} + \gamma\ \text{grad}\ V = 0\ , \tag{1}$$

$$\text{div}\left(\gamma\ \frac{\partial \mathbf{A}}{\partial t} + \gamma\ \text{grad}\ V\right) = 0\ . \tag{2}$$

In the domains Ω_2 and Ω_3, the electromagnetic field is described by the equation

$$\text{rot}\ (\mu^{-1}\ \text{rot}\ \mathbf{A}) = \mathbf{J}^{\text{ext}}\ . \tag{3}$$

At the boundary $\Gamma_{n,c}$ of contact between the electrically conductive (Ω_1) and dielectric (Ω_2) domains, we specify boundary conditions of continuity for the tangential component of the magnetic field strength and of continuity for the normal component of the magnetic induction:

$$\mu_1^{-1}\ \text{rot}\ \mathbf{A}_1 \times \mathbf{n} = \mu_2^{-1}\ \text{rot}\ \mathbf{A}_2 \times \mathbf{n}\ , \tag{4}$$

$$\text{rot}\ \mathbf{A}_1 \cdot \mathbf{n} = \text{rot}\ \mathbf{A}_2 \cdot \mathbf{n}\ . \tag{5}$$

Analogously we write the conditions at the boundary between the domains Ω_2 and Ω_3. Condition (4) yields that on abrupt change in the magnetic permeability, the function **A** must be discontinuous at the boundary $\Gamma_{n,c}$.

At the external boundary Γ_n of the dielectric domain Ω_2, we specify the condition of parallelism or perpendicularity for the magnetic induction (depending on the problem in question):

$$\text{rot}\ \mathbf{A} \cdot \mathbf{n} = 0\ , \tag{6}$$

$$\text{rot}\ \mathbf{A} \times \mathbf{n} = 0\ . \tag{7}$$

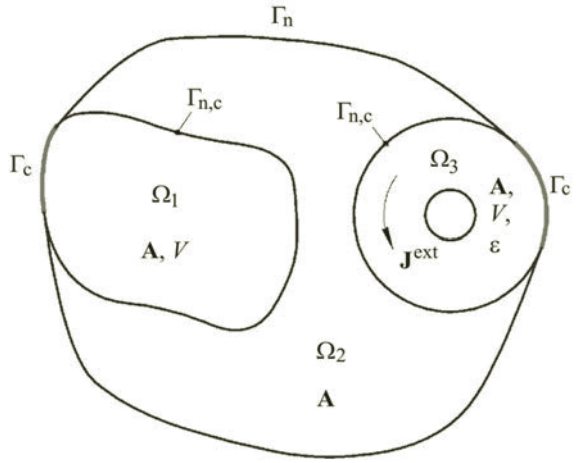

Fig. 1. Domain in the space of modeling of an electromagnetic field.

In the planes of symmetry of the analyzed domain, there can be the external boundaries Γ_c of the electrically conductive domains Ω_1 and Ω_3 (Fig. 1). In the case of the perpendicularity of the eddy currents to these planes, the boundary conditions are of the form

$$\mathbf{A} \times \mathbf{n} = 0 , \tag{8}$$

$$V = \text{const} . \tag{9}$$

The density vector of the eddy currents **J** (A/m^2) is calculated from the formula

$$\mathbf{J} = -\gamma \frac{\partial \mathbf{A}}{\partial t} - \gamma \text{ grad } V . \tag{10}$$

Consequently, the condition of parallelism of the eddy currents to the planes of symmetry has the form

$$\mathbf{n} \cdot \left(\gamma \frac{\partial \mathbf{A}}{\partial t} + \gamma \text{ grad } V \right) = 0 . \tag{11}$$

Approximation of the vector magnetic potential is carried out from the equation [7]

$$\mathbf{A} \approx \sum_{k=1}^{n_e} a_k N_k . \tag{12}$$

The electric potential is approximated by the nodal basis functions:

$$V \approx \sum_{k=1}^{n_n} V_k N_k . \tag{13}$$

Solution of mathematical model (1)–(11) in the ANSYS system is realized using 20-node finite elements SOLID236. The integral of the vector magnetic potential along the edge of the element a_k in the ANSYS system is denoted by AZ, and the scalar electric potential, by VOLT. Subdividing the model into subdomains enables us to minimize the total number of unknowns: Eq. (3) is only solved for the vector magnetic potential. Thus, the existence domain of eddy currents Ω_1 is approximated by the finite elements SOLID236 with degrees of freedom AZ for each edge and VOLT for each node. The domains Ω_2 and Ω_3 contain finite elements with degree of freedom AZ.

Direct use of Eq. (3) is only possible in the cases of a determinate current density in inductors. In actual practice, we more often face the problem of connection of the inductors to a voltage source. The voltage drop on the inductor is expressed by the equation

$$\Delta V = RI + \varepsilon \, . \tag{14}$$

The self-induction electromotive force (EMF) is determined by the rate of change in the magnetic flux Φ through the inductor:

$$\varepsilon = \frac{d\Phi}{dt} = \frac{N_c}{S_c} \int\limits_{\Omega_3} \mathbf{t} \, \frac{d\mathbf{A}}{dt} \, d\Omega \, . \tag{15}$$

The inductor is usually modeled more simply, i.e., as a solid (continuous) body. In [9], it has been shown that the layout of turns, and also gaps between them exert no influence on induced eddy currents. Consequently, the averaged current density for the inductor′s simplified model will be

$$\mathbf{J}^{\text{ext}} = \mathbf{t} \cdot IN_c/S_c \, . \tag{16}$$

With account of expressions (13) and (15), Eq. (3) for the case of connection of the inductor to the voltage source will be rewritten in the following form:

$$\text{rot} \, (\mu^{-1} \, \text{rot} \, \mathbf{A}) = \mathbf{t} \cdot IN_c(\Delta V - \varepsilon)/(S_c R) \quad . \tag{17}$$

The inductor connected to the voltage source is modeled in the ANSYS system using the finite elements SOLID236 with degrees of freedom AZ, VOLT, and EMF. The voltage drop ΔV is assigned as the degree of freedom VOLT at all the nodes. In this connection, contact of the domains Ω_1 and Ω_3 cannot be allowed; an insulator in the form of Ω_2 between them is needed, which prevents the "flowing" of the scalar electric potential V through the shared nodes with degree of freedom VOLT to the existence domain of eddy currents Ω_1. The values of the degrees of freedom EMF are taken identical for all the inductor nodes.

The mathematical model based on the edge vector current potential **T** and on the nodal magnetic scalar potential φ is distinguished by less exacting requirements of computational resources, however, ranks behind model (1)–(11) as far as calculation accuracy is concerned [4, 10]. In the present work, this formulation is not considered and relations (1)–(11) realized in the ANSYS system are used to model the eddy currents.

Since the magnetic permeability of a ferromagnetic material depends in the magnetic field strength, solution of nonlinear differential equation (1) takes much computer time, which is particularly critical when the electromagnetic processes in question are nonstationary. Under the assumption of the constant magnetic permeability and the sinusoidal voltage source, Eq. (1) is much simplified to a linear quasi-steady equation in complex representation:

$$\mu^{-1} \, \text{rot} \, (\, \text{rot} \, \dot{\mathbf{A}}) + j2\pi j\gamma \dot{\mathbf{A}} + \gamma \, \text{grad} \, \dot{V} = 0 \, .$$

Equations (2)–(11) are rewritten analogously.

Calculating a constant value of magnetic permeability that is equivalent to the magnetization curve, as far as the criterion of active power is concerned, is based on a nonlinear two-dimensional electromagnetic analysis. In a two-dimensional formulation, on condition that the external current is perpendicular to the XY plane, the magnetic vector potential has the only component A_z are there is no need for introduction of the scalar electric potential. Thus, vector equation (1) is simplified to a scalar equation:

$$\text{rot} \, (\mu^{-1} \, \text{rot} \, A_z) + \gamma \, \frac{\partial A_z}{\partial t} = 0 \, . \tag{18}$$

Solution of nonlinear equation (18) presents no computational problems. Therefore, the two-dimensional formulation can efficiently be used to calculate the equivalent magnetic permeability. This procedure has been presented in [7] in greater detail. A result of the solution of the electromagnetic problem is the field of heat releases in the plate′s volume $q = q(x, y, z)$ at the instant of time t, which is used to solve the heat-conduction equation

$$\frac{\partial T}{\partial t} = \frac{\lambda}{c\rho} \nabla^2 T + \frac{q}{c\rho} \, . \tag{19}$$

The heat release is determined according to the Joule–Lenz law

$$q = |J|^2/2\gamma \, . \tag{20}$$

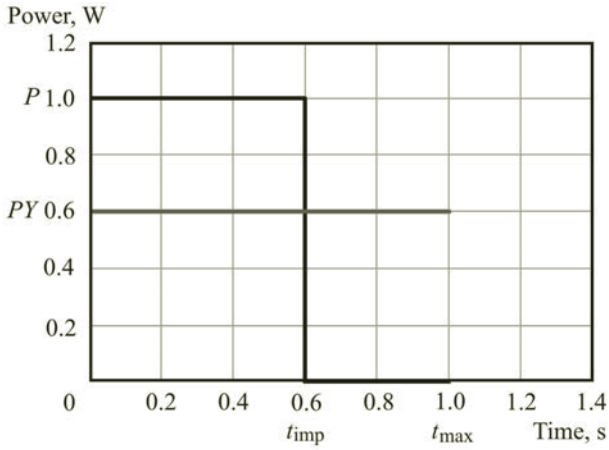

Fig. 2. Control pulsed signal and its approximation.

The initial condition for Eq. (19) is as follows:

$$T(x, y, z, 0) = T_0 \ . \tag{21}$$

The heat transfer from the working surface, the cover, and the ends of a heating plate, and also from the lateral surfaces of molds in the absence of heat insulation is described by the boundary conditions of the third kind

$$-\lambda \left.\frac{\partial T}{\partial n}\right|_{\Omega_{p,r}} = \alpha_r (T_r - T_{\text{amb}}) \ . \tag{22}$$

The coefficients of heat transfer from the rth surface (of a plate, a mold) α_r is determined with criterial equations according to [11].

Procedures of Calculation of the Temperature Fields of Induction Heating Devices at the Stage of Automatic Control. The implementation of the processes of vulcanization of RTGs or heat treatment of plastics involves the stage of holding at an exactly defined temperature. To control heating devices using the PID law, use is most frequently made of pulse-width control: the controller′s output signal Y taking on values in the range from 0 to 1 is converted to a pulse whose duration (width) is

$$t_{\text{imp}} = t_{\max} Y \ . \tag{23}$$

At this moment, voltage is fed to the heaters. Next, during the period $t_{\max} - t_{\text{imp}}$, the heaters are disconnected, and thereafter a new control signal is generated. Fast action of today′s controllers makes it possible to update the control signal with a period of tens of milliseconds. In this connection, the implementation of a mathematical model simulating the actual operation of a PID controller takes much computer time. For example, modeling a holding period of duration 30 min at the value $t_{\max} = 1$ s will require 3600 computational time steps (two steps per $t_{\max}$). With a modern computer, such thermal analysis may last for tens of hours.

To reduce the consumption of computer time in calculating the temperature field at the stage of PID-controlled holding, we propose the following approach. The period $t_{\max}$ with a stepwise change in the power from the rated power P to 0 is approximated by a constant value of PY (Fig. 2). Here, instead of the constant computational time step $t_{\max}$, we use a variable step whose value is determined from an analysis of the second derivative of the temperature of a checking thermocouple: the step increases if the change in the thermocouple′s control temperature approaches a linear law [12]. Thus, this model approximately reproduces the operation of an actual PID controller from the value of the average control action, which finally forms a temperature field. Note that the tuning factors of the modeled and actual PID controller may differ significantly because of the different value of time steps. If the modeling seeks to determine the factors of the PID controller, we should use a constant step (period of updating of the control signal), and also its computation algorithms which are usually not given in the instruction manuals of the manufacturer of the controller and is proprietary information (algorithm of computation of an antisaturating correction, etc,).

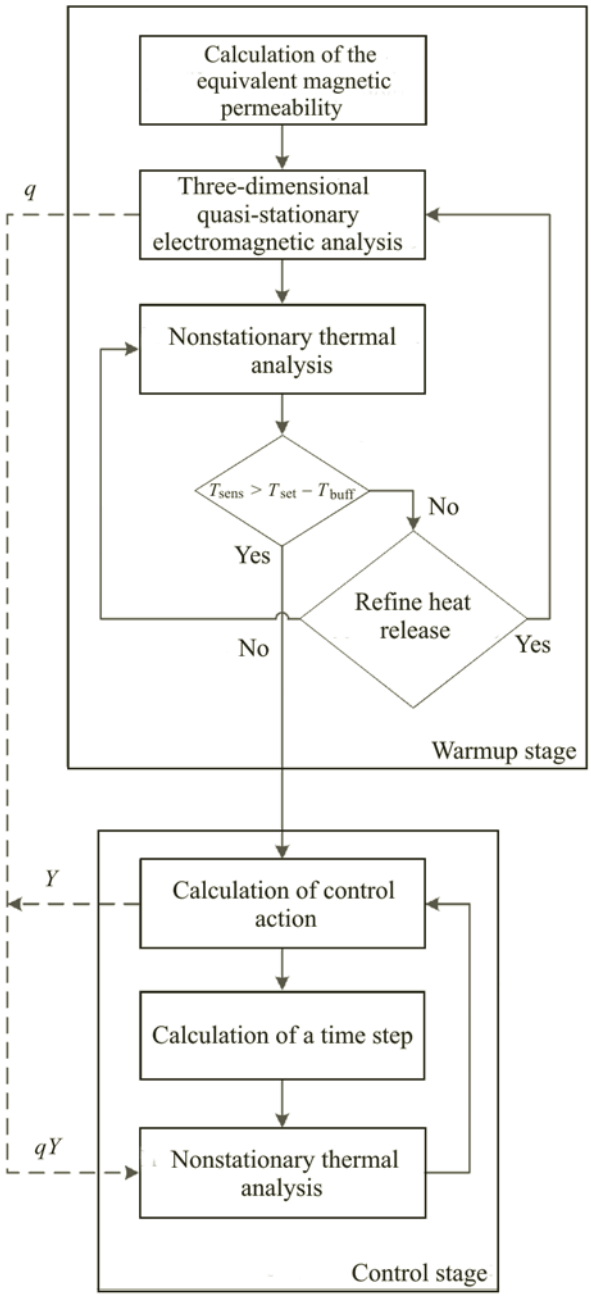

Fig. 3. Complete diagram of calculation of the temperature fields of induction heating devices including the calculation of three-dimensional eddy-current fields.

Figure 3 gives the diagram of the procedure of calculation of the temperature fields of induction heating devices, which includes the calculation of three-dimensional fields of eddy currents. At the warmup stage at a constant rated power, it is unexpedient to use the model of a PID controller. The controller is "switched on" when the condition $T_{sens} - T_{buff}$ is observed. The use of a "buffer zone" of T_{buff} enables us to avoid excessive correction (overcontrol). Practical calculations suggest that the optimum value of T_{buff} lies in the range 5–15 K.

Since the electrical conductivity of materials decreases in the process of heating, the overall heat-release power gradually decreases. Dissimilar time scales of electromagnetic and thermal processes make it difficult to simultaneously solve Eqs. (1)–(11) and (18). At an industrial frequency of the electric current of 50 Hz, the period of its oscillations is 20 ms. Consequently, to adequately describe nonstationary electromagnetic processes, a time step must be no longer than 2

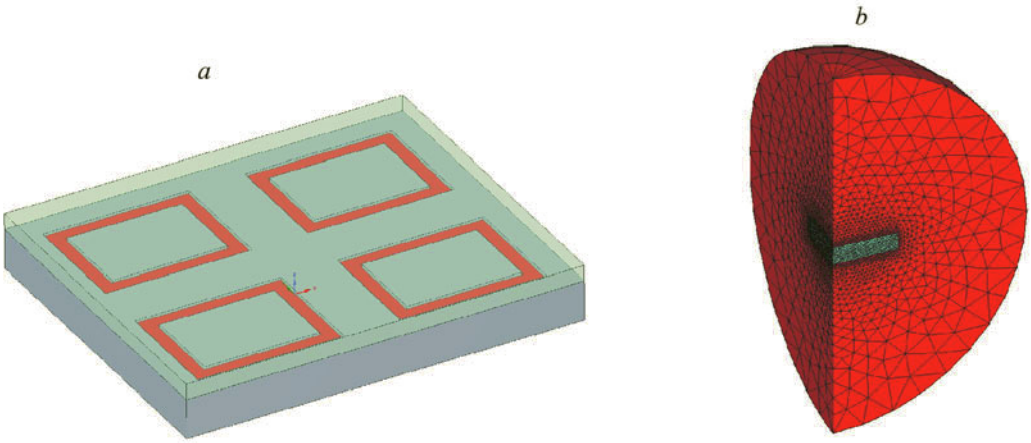

Fig. 4. Model of an induction-heating plate: a) geometry of the plate with four inductors and b) finite-element grid of the computational domain.

ms, which, under the conditions of slow thermal processes, leads to an excessive amount of computations. Rough estimation of the consumption of computer time shows that simultaneous solution of the equations of the electromagnetic and thermal models of induction heating of an actual plate will take no less than three years (on a 1 min per time step basis at a final heating time of 60 min). Therefore, a successive type of analysis is used to model induction heating (Fig. 3).

In [13], it has been shown that acceptable accuracy of calculating temperature fields with the successive type of analysis is attained, if the average plate temperature increases by no more than 50°C in the course of one iteration. For example, if the initial plate temperature is 20°C, and the final one, 150°C, no less than three iterations of electromagnetic analysis are necessary. Consequently, no solution of the equations of the electromagnetic model at each new stage of control is required. The heat-release field q calculated at the last iteration of electromagnetic analysis from Eq. (19) is "scaled" in accordance with the controller′s output signal. For the ith time step, we have the equality

$$q_i = Y_i q \ . \tag{24}$$

Figure 4 gives the model of a commercial induction-heating plate, which is used for RTG production. The grid of finite elements of the electromagnetic model includes the elements of surrounding air space on whose spherical exterior surface condition (6) is specified. The grid of finite elements of the thermal model consists of just the plate elements and the inductor and the insulator between them.

Passage to linear differential equations of the electromagnetic field considerably simplifies the problem, but solving them in a three-dimensional formulation requires extensive computational resources. For example, approximately 8 Gb of random-excess memory and 2 h of computer time (AMD Phenom II X4 920 processor) are required to calculate the field of eddy currents in the model of a quarter of the heating plate, which includes 730 thousand finite elements (Fig. 4a). An analysis of electromagnetic and thermal processes in the system "plate–mold–product" assumes considering a model of two plates between which there are molds with products. Thus, the problem′s resource intensity increases more than twofold for a single plate.

An alternative approach to solution of such a problem (Fig. 5) is in modeling the temperature fields under the assumption of a uniform release of heat in the inductor domain Ω_3:

$$q = P_{\text{ind}} / V_{\text{ind}} \ . \tag{25}$$

This approach is inconsistent with the physics of the process of induction heating: heat is released in the volume of the plate at the boundary with the inductors, not in the inductors. However, at a relatively high thermal conductivity of the plate′s material, the temperature gradient is smoothed out in accordance with Fourier′s law. Thus, in the majority of cases, the difference in heat-release distribution is reflected only slightly on the final result: the temperature field on the working surface of the heating plate and in the product, which is partly confirmed by the conclusions in [3]. At the stage of automatic

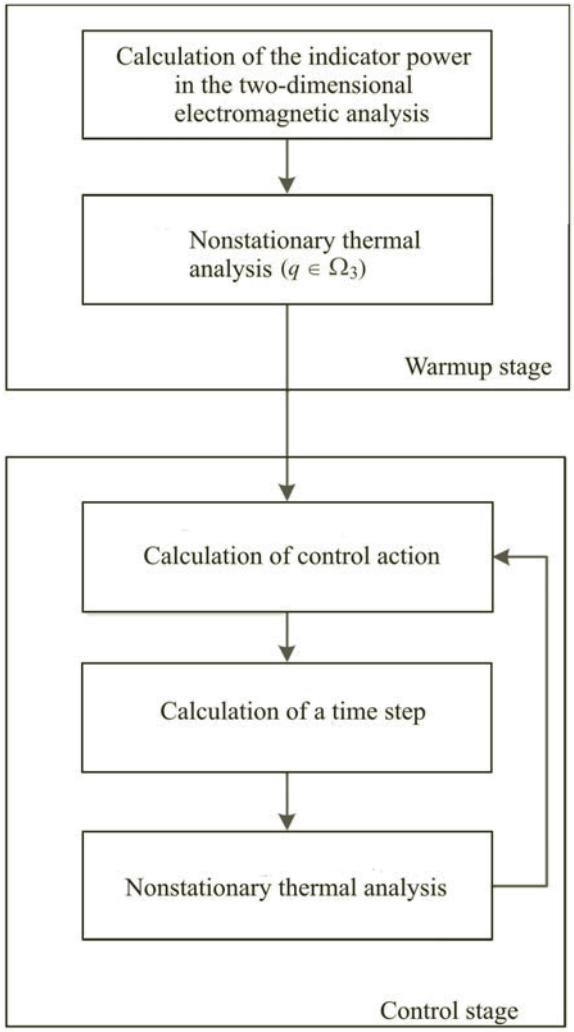

Fig. 5. Diagram of the simplified procedure of calculation of the temperature fields of induction heating devices which includes only a nonstationary thermal analysis.

control, the average power considerably decreases to a level corresponding to the heat loss. Consequently, the values of heat fluxes inside the plate decrease, which leads to an equalization of the temperature field. This effect additionally diminishes the influence of the localization of heat releases on the final result.

For calculating the inductor power P_{ind}, we propose the following procedure. The initial three-dimensional inductor is approximated by a two-dimensional axisymmetric model from the condition of equality of the lengths of their axial lines:

$$R_{2D} = L_{3D}/2\pi \,. \tag{26}$$

Here, the geometry of the cross section of a groove for an inductor remains constant. As noted above, in two-dimensional formulation (18), taking account of the magnetization curve presents no problems. Consequently, the inductor power average over the period can be calculated with a high degree of accuracy according to the equation

$$P_{\text{ind}} = f \int_{t_{\text{st}}}^{t_{\text{st}}+1/f} \int_{\Omega_1} \frac{J_z^2}{\gamma} \, d\Omega \, dt \,, \tag{27}$$

where the eddy-current density is determined from the formula

$$J_z = -\gamma \frac{\partial A_z}{\partial t} \,. \tag{28}$$

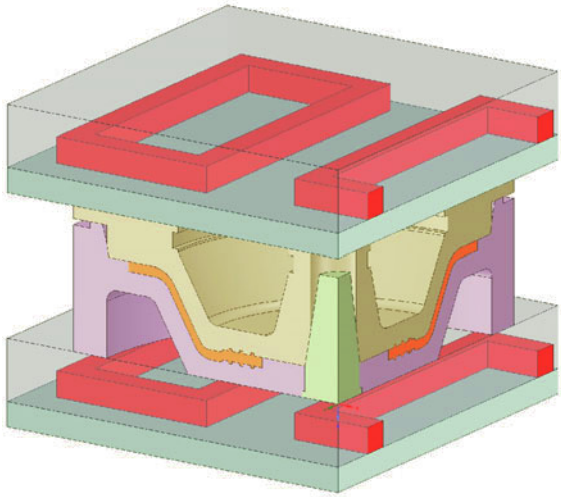

Fig. 6. Geometry of a quarter of the calculated system "plate–mold–product."

The choice of the axisymmetric model is due to the possibility of placing several inductors of varying length in one plate, and also to the reproduction of an "annular effect" which is manifested in the domains of the current reversal: the induction of the magnetic field inside the annulus is higher than outside. A more detailed presentation of the procedure and its substantiation and the field of application are given in [9].

Example of Practical Use of the Simplified Procedure. With the simplified procedure of modeling of induction heating, we have carried out a calculation of the system "plate–mold–product" whose objective was to determine the temperature difference in the product′s volume during the period of vulcanization. Figure 6 gives the geometry of a quarter of the calculated system: use is made of the model of a plate of total average power 6080 W with six inductors controlled by one PID controller. Between the plates, there is a mold to fabricate a membrane, which consists of three plates.

Under the regulations, the plates and empty molds are warmed up, until an assigned temperature T_{set} is attained at the site of installation of the checking thermocouple. Next, the plates are released, and a rubber mixture is charged into the molds. Thereafter, a stage of press molding is implemented during the scheduled vulcanization time. The vulcanization temperature of a rubber mixture is usually taken as T_{set} (in the example, $T_{set} = 151^{o}$C). Due to the difficulty with formalizing, the processes of releasing the plates and charging the rubber mixture were not modeled: the assumption was made that the charging is instantaneous when the condition $T_{sens} > T_{set} - 1$ is observed.

Figure 7a gives the graphs of behavior of the plate temperature at the site of installation of the checking thermocouple and of the temperature of the product charged at an instant of time of 2645 s. Under the regulations, vulcanization of the membrane lasts for 20 min. After this time interval, the temperature average over the product′s volume was only 142.6^{o}C. The vulcanization temperature of the rubber mixture (151^{o}C) is attained within 39 min after the charging (Fig. 7b). The graph of behavior of the power of the plate is given in Fig. 8b. In a time interval of 2560–5000 s, the plate′s power continuously decreases without reaching a steady-state value.

In designing new plates and analyzing the existing structures, the dynamics of the temperature difference over the working surface (Fig. 8a) is of particular interest. At the stage of warmup, the temperature difference increased to a value of 37.6% at the maximum power. Decrease in the power at the stage of automatic control (Fig. 7b) leads to an equalization of the temperature field. The presence of the minimum on the graph of the temperature difference (3.0^{o}C at an instant of time of 4500 s) is attributed to the distinctive feature of the heating-plate structure: at the maximum power, the peripheral region is heated faster than the central part. Figure 9a gives the temperature field of a quarter of the plate′s working surface on completion of the warmup stage. The temperature minimum corresponds to the center of the plate, and the maximum, to the corner region. On reduction in the power, the center of the plate is gradually warned up because of the high thermal conductivity of the plate′s material. By an instant of time of 5000 s, the field pattern is reversed: the temperature maximum shifts to the center of the plate, and the minimum, to its corner (Fig. 9b). Thus, the extremum on the graph of the temperature difference is characterized by the equilibrium of the temperatures of the corner and central regions of the plate. Warming up the center of the plate requires an energy whose expenditure decreases as the temperature grows, which explains the gradual reduction in the power consumption of the plate at the stage of automatic control.

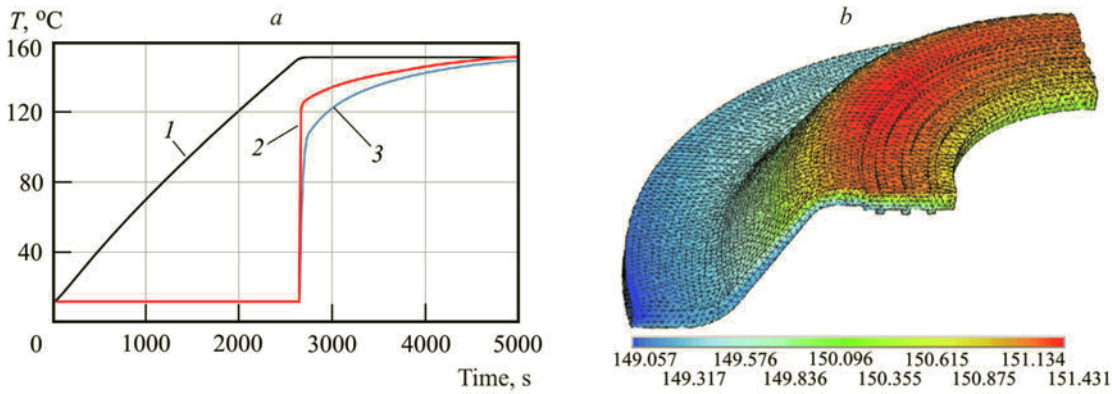

Fig. 7. Temperature of the product and of the checking thermocouple: a) graphs of the temperature at the site of installation of the checking thermocouple (1), maximum temperature of the product (2) and minimum temperature of the product (3) and b) temperature field of a quarter of the product at a final instant of time of 5000 s.

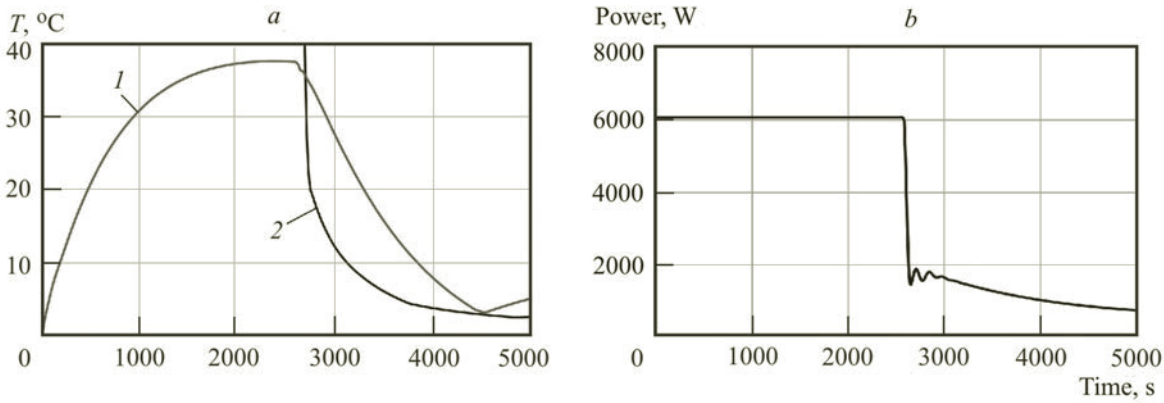

Fig. 8. Temperature differences and power of the plate vs. time: a) graphs of temperature differences on the plate surface (1) and over the product's volume (3) and b) power consumed by the plate.

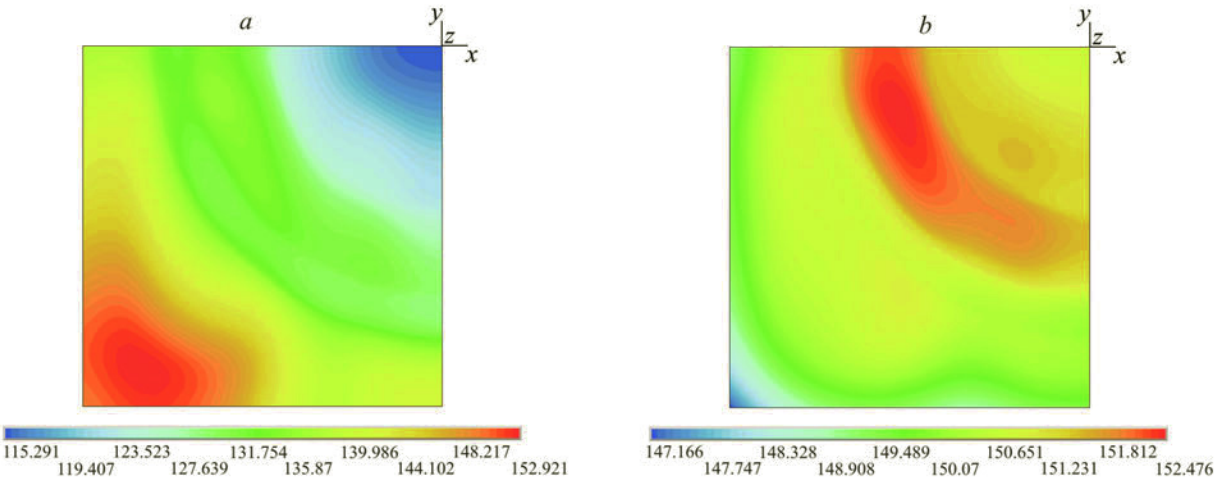

Fig. 9. Temperature field of a quarter of the working surface of the plate (its center corresponds to the top right corner) at different instants of time: a) 2525 and b) 5000 s.

An analysis of the calculation result allows the conclusion on the necessity of singling out a stage of stabilization of the temperature field: on completion of warming up, the temperature field of the heating plate and hence of the mold fails to meet technical requirements of the process of vulcanization. Stabilization of the temperature field requires a certain time, which depends on the plate structure. For the considered example, this time was approximately 25 min.

The use of the simplified procedure of calculation of the temperature fields of induction heating devices enabled us to obtain a solution with a minimum consumption of computer time. The calculation of the warmup stage lasted for 14 min, and the calculation of the automatic-control stage, for 109 min. The total number of time steps was 170. Since the electromagnetic analysis requires a small step of discretization of space near magnetic-field sources, eliminating three-dimensional equations of an electromagnetic field made it possible to significantly reduce the number of finite elements. The model′s geometry given in Fig. 5 was approximated by 581,033 finite elements.

Conclusions. To solve the problem of calculating temperature fields of press equipment in induction heating, the choice was made in favor of a mathematical model based on the edge vector magnetic potential and the nodal scalar electric potential, which ensures high accuracy of solution.

Two procedures have been proposed to calculate temperature fields of induction heating plates at the stage of automatic PID control, which make it possible to considerably reduce the amount of computations. According to the first procedure, heat releases from eddy currents at each time step are determined as a result of the "scaling" of the heat releases calculated earlier at the stage of warmup using linear differential equations of the electromagnetic field. This approach enables us to use a variable time step without the need for multiple solution of electromagnetic-field equations.

The second procedure is based on the assumption of a uniform release of heat in the region of grooves for inductors, which allows reducing the problem of electromagnetic analysis to a problem of determination of the inductor power, which can be solved in a two-dimensional formulation. It is expedient to use this procedure under the conditions of shortage of computational resources; however, the issue of occurring errors in calculating the temperature fields when the heat releases are represented more simply remains open.

With the proposed procedures, an analysis has been made of the system "plate–mold–product" at the stages of warmup and automatic PID control. Calculation results showed the necessity of singling out and taking account of the stage of stabilization of a temperature field in designing new plates and operating the existing ones. In the considered example, early charging of the product leads to insufficient heating, which may cause rejection. Also, such calculations enable us to make a justified choice of the site of installation of a checking thermocouple and an assigned value of its temperature to ensure required temperature modes in the product.

Acknowledgment. This work was carried out with financial support from the Ministry of Education and Science of the Russian Federation within the framework of the basic part (Project No. 8.7082.2017/8.9).

NOTATION

A, vector magnetic potential, Wb/m; A_z, z component of the vector magnetic potential, Wb/m; a_k, curvilinear integral of the vector magnetic potential **A** along the edge k of the finite element; c, heat capacity of the plate′s material, $J \cdot kg^{-1} \cdot K^{-1}$; f, oscillation frequency of the voltage source, Hz; I, inductor current, A; **J**, vector of the eddy-current density, A/m^2; J_z, z component of the vector of the eddy-current density, A/m^2; $\mathbf{J}^{ext}$, current density of the external source, A/m^2; $|J| = \sqrt{\mathrm{Re}\ \dot{J}^2 + \mathrm{Im}\ \dot{J}^2}$, modulus of the complex amplitude current density; j, imaginary unit; L_{3D}, length of the initial inductor along the axial line, m; N_k, basis function for the edge k; N_c, number of turns of the inductor; **n**, unit vector of the normal to the surface of contact between the electrically conductive and dielectric domains; n_e, number of edges of a finite element; n_n, number of nodes of a finite element; P_{ind}, inductor power, W; q, field of heat releases, W/m^3; R, ohmic resistance of the inductor, Ω; R_{2D}, average radius of the axisymmetric analog of the initial inductor, m; S_c, area of the inductor cross section, m^2; **T**, edge vector current potential, A/m; $T = T(x, y, z)$, temperature at a point of the plate volume with coordinates (x, y, z) at the instant of time t, K; T_0, plate temperature at the initial instant of time t, K; T_r, average temperature of the rth plate surface, K; T_{amb}, ambient-air temperature, K; T_{buff}, difference between the assigned plate temperature and the temperature of the beginning of the control stage ("buffer zone"), K; T_{sens}, temperature at the site of installation of the checking thermocouple, K; T_{set}, assigned value of the operating plate temperature, K; **t**, unit vector of the direction of the current in the inductor; t, time, s; t_{imp}, duration of a pulse to which the controller output signal is converted, s; t_{max}, maximum pulse width (period of generation of control signals), s; t_{st}, conditional time of stabilization of electromagnetic processes, after which the changes in the amplitude values of the current density J_z may be ignored, s; V, scalar electric potential, V; V_k, value of the scalar electric potential at the node k; V_{ind}, volume of a groove to place an inductor, m^3; Y, controller′s output signal taking on values in the

range from 0 to 1; α_r, coefficient of heat transfer from the rth surface, $W \cdot m^{-2} \cdot K^{-1}$; γ, specific electrical conductivity, $\Omega^{-1} \cdot m^{-1}$; ε, self-induction electromotive force, V; Φ, magnetic flux through the inductor, Wb; φ, nodal magnetic scalar potential, A; λ, thermal conductivity of the plate′s material, $W \cdot m^{-1} \cdot K^{-1}$; μ, magnetic permeability, H/m; ρ, density of the plate′s material, kg/m^3; $\Omega_{p,r}$, rth surface of the heating plate or of the mold. Subscripts and superscripts: 2D, two-dimensional; 3D, three-dimensional; amb, ambient, buff, buffer; c, coil; ext, external; e, edge; ind, inductor; imp, impulse, pulse; sens, sensor; set, setting (assigned value of the checking-thermocouple temperature).

REFERENCES

1. E. N. Malygin, S. V. Karpushkin, and S. V. Karpov, Modeling and calculation of the processes of induction heating of press equipment in the production of rubber technical goods, *Nauka Obraz. Élektron. Nauch. Tekh. Izd*., No. 3, 85–104 (2013); DOI: 10.7463/0313.0541632.
2. D. Selvakarthi, S. J. Suji Prasad, R. Meenakumari, and P. A. Balakrishnan, Optimized temperature controller for plastic injection molding system, *2014 Int. Conf. on Green Computing Communication and Electrical Engineering (ICGCCEE)* — IEEE, No. 1, 977–981 (2014).
3. X. G. Hou and C. L. Wang, Induction heating furnace temperature control based on the fuzzy PID, *Appl. Mech. Mater*., **217–219**, 2463–2466 (2012).
4. C. J. Carpenter, Comparison of alternative formulations of 3-dimensional magnetic-field and eddy-current problems at power frequencies, *Proceedings of the Institution of Electrical Engineers*; https://doi.org/10.1049/piee.1977.0211.
5. R. Plasser, G. Koczka, and O. Bíró, A nonlinear magnetic circuit model for periodic eddy current problems using T, Φ–Φ formulation, *COMPEL — The Int. J. Comput. Math. Electr. Electron. Eng.*, **36**, No. 3, 649–664 (2017).
6. O. Bíró and K. Preis, On the use of the magnetic vector potential in the finite-element analysis of three-dimensional eddy currents, *IEEE Trans. Magn*., **25**, No. 4, 3145–3159 (1989); https://doi.org/10.1109/20.34388.
7. O. Bíró, Edge element formulations of eddy current problems, *Comput. Methods Appl. Mech. Eng.*, **169**, Nos. 3–4, 391–405 (1999); https://doi.org/10.1016/S0045-7825(98)00165-0.
8. A. Kameari, Calculation of transient 3D eddy current using edge-elements, *IEEE Trans. Magn*., **26**, No. 2, 466–469 (1990); https://doi.org/10.1109/20.106354.
9. S. Karpushkin, A. Glebov, and S. Karpov, Calculation of equivalent magnetic permeability of ferromagnetic materials for modeling of three-dimensional eddy current fields, *MATEC Web Conf.* (2017); https://doi.org/10.1051/matecconf/201712902006.
10. A. Candeo, C. Ducassy, P. Bocher, and F. Dughiero, Multiphysics modeling of induction hardening of ring gears for the aerospace industry, *IEEE Trans. Magn*., **47**, No. 5, 918–921 (2011).
11. P. G. Romankov, V. F. Frolov, O. M. Flisyuk, and M. I. Kurochkina, *Methods for Calculating Processes and Apparatuses of Chemical Technology* [in Russian], Khimiya, Leningrad (1988).
12. A. O. Glebov, S. V. Karpov, S. V. Karpushkin, and M. N. Krasnyanskii, Development and investigation of mathematical models of a system for automatic control over the temperature of heating plates of a vulcanizing press to fabricate rubber technical goods, *Prib. Sist. Upravl. Kontrol' Diagnostika*, No. 11, 33–44 (2013).
13. A. O. Glebov, S. V. Karpov, and S. V. Karpushkin, A comparison of modeling techniques for temperature fields of inductive heating plates, *Autom. Remote Control*, **75**, No. 6, 1120–1129 (2014).